Photosynth Res (2016) 128:93–102
DOI 10.1007/s11120-015-0205-y

ORIGINAL ARTICLE

Native FMO-reaction center supercomplex in green sulfur bacteria: an electron microscopy study

David Bína[1,2] · Zdenko Gardian[1,2] · František Vácha[1,2] · Radek Litvín[1,2]

Received: 31 August 2015 / Accepted: 12 November 2015 / Published online: 20 November 2015

Abstract *Chlorobaculum tepidum* is a representative of green sulfur bacteria, a group of anoxygenic photoautotrophs that employ chlorosomes as the main light-harvesting structures. Chlorosomes are coupled to a ferredoxin-reducing reaction center by means of the Fenna–Matthews–Olson (FMO) protein. While the biochemical properties and physical functioning of all the individual components of this photosynthetic machinery are quite well understood, the native architecture of the photosynthetic supercomplexes is not. Here we report observations of membrane-bound FMO and the analysis of the respective FMO-reaction center complex. We propose the existence of a supercomplex formed by two reaction centers and four FMO trimers based on the single-particle analysis of the complexes attached to native membrane. Moreover, the structure of the photosynthetic unit comprising the chlorosome with the associated pool of RC-FMO supercomplexes is proposed.

Keywords FMO (Fenna–Matthews–Olson protein) · Chlorosome · Light-harvesting complex · Reaction center · Electron microscopy · Green sulfur bacteria

Abbreviations

BChl	Bacteriochlorophyll
C.	*Chlorobaculum*
Cfx.	*Chloroflexus*
CSM	Chlorosome
FMO	Fenna–Matthews–Olson protein
GSB	Green sulfur bacteria
gRC	Reaction center of green sulfur bacteria
PSI RC	Reaction center of photosystem 1 of oxygenic photosynthesis
RC	Reaction center
TEM	Transmission electron microscopy

✉ David Bína
bina@umbr.cas.cz

[1] Faculty of Science, University of South Bohemia, Branišovská 1760, 370 05 České Budějovice, Czech Republic

[2] Institute of Plant Molecular Biology, Biology Centre CAS, Branišovská 31, 370 05 České Budějovice, Czech Republic

Introduction

Green sulfur bacteria (GSB, *Chlorobiaceae*) are photoautotrophic inhabitants of aquatic anoxic environments, both planktonic and benthic, that utilize reduced sulfur compounds as electron donors for photosynthesis (van Gemerden and Mas 1995). The light-driven charge separation is performed by a reaction center (RC) which is of type I. Compared to photosystem I (PSI), the structure of the GSB RC (gRC) appears simpler, consisting of five subunits only: a homodimer of PscA protein comprising 11 transmembrane helices that is homologous to the PsaA/B heterodimer of PSI RC; PscB, binding the iron-sulfur (Fe-S) clusters; cytochrome subunit PscC; and PscD, presumably functioning in ferredoxin docking, RC stabilization and excitation energy transfer (Hauska et al. 2001; Tsukatani et al. 2004). Despite the apparent similarity of the protein scaffold, there is a marked difference in the pigment complement between the PSI RC and gRC. While the core of the PSI binds nearly 100 Chl *a* molecules, the PscA dimer of GSB binds only ~20 chlorins, both bacteriochlorophyll (BChl) *a* and chlorophyll (Chl) *a*. This relative deficiency in pigment content is more than compensated for by the unique external

antenna, the chlorosome (CSM), a large ellipsoidal structure formed by self-assembling aggregates of $\sim 10^5$ of BChl's (*c*,*d*,*e*), carotenoids and quinones, surrounded by a lipid monolayer containing integral proteins (Orf and Blankenship 2013). The BChl body rests upon a paracrystalline aggregate of a small BChl *a*-binding protein (CsmA), the baseplate. The link between the gRC and the chlorosome is formed by a homotrimeric BChl *a*-binding pigment-protein complex, the Fenna–Matthews–Olson protein (FMO).

The first chlorophyll-binding protein to have its structure determined to atomic resolution (Fenna and Matthews 1975; Tronrud et al. 1986), FMO has been a subject of numerous experimental and theoretical studies. A large part of this body of work was dedicated to structure-based interpretation of optical spectra. However, in spite of the longstanding interest, the FMO protein has retained certain somewhat mysterious aspects. Its total pigment complement, 8 BChl *a* per monomer, was conclusively determined only recently (Tronrud et al. 2009; Wen et al. 2011) and the contribution of the last discovered (8th) BChl *a* to the spectroscopic properties of the complex has been so far analyzed almost exclusively on the theoretical level (Olbrich et al. 2011; Schmidt am Busch et al. 2011; but see Bina and Blankenship 2013). The FMO complex also exhibits a redox-dependent fluorescence quenching, likely a relevant in vivo regulatory process (Zhou et al. 1994; Hohmann-Marriott and Blankenship 2007a), of unknown mechanism. Thirdly, the native stoichiometry of the FMO-gRC complex cannot be considered a solved issue. Different purification and quantification approaches yielded a broad range of plausible stoichiometries between 1 and 8 FMO per gRC (e.g., Swarthoff and Amesz 1979; Griesbeck et al. 1998; Remigy et al. 1998, 1999; Frigaard et al. 2003). Arguably, the best supported appears to be the binding of 2 FMO trimers per 1 gRC complex, that has even been observed directly by electron microscopy (Remigy et al. 1999), which however does not preclude a different in vivo stoichiometry, possibly involving a combination of strongly and loosely bound FMO trimers. It is known that FMO is in contact with the RC subunits PscB and D that are located near the center of the gRC complex and that FMO-PscD interaction affects the energy transfer from the FMO to the gRC core (Remigy et al. 1999; He et al. 2014; Tsukatani et al. 2004). Last but not least, the question of mechanism of formation in vivo of the remarkable natural nanostructure of the RC-CSM complex remains open (Sprague et al. 1981; Hohmann-Marriott and Blankenship 2007b; Pedersen et al. 2010; Psencik et al. 2014).

The higher order organization of the photosynthetic apparatus remains little studied, in marked contrast to purple photosynthetic bacteria (for review see e.g., Scheuring et al. 2005, for more recent development, e.g., Cartron et al. 2014 and references therein) and even filamentous anoxygenic phototrophs, *Chloroflexi* (Bina et al. 2014, Majumder et al. 2015), although several insightful whole-cell electron-microscopic studies are available (Hohmann-Marriott et al. 2005; Kudryashev et al. 2014; also see Oelze and Golecki 1995). Nevertheless, the available data allow formulation of testable hypotheses concerning the placement of FMO and gRC with respect to the CSM baseplate. Two limiting cases can be envisioned: the baseplate serves as the organizing center for the FMO, which could form a regularly structured layer stretching along the whole baseplate (Frigaard et al. 2003) to which are the gRC complexes anchored via the firmly bound FMO trimer(s). In this case, the total FMO:RC stoichiometry might not be precisely defined. The resulting positioning of gRC could be also regular, although the available spatial data indicate disordered gRC geometry (Kudryashev et al. 2014), mimicking the situation in the CSM-containing *Chloroflexi* (Bina et al. 2014). Alternatively, the FMO might be organized primarily by interaction with the gRC complex, with a well-defined stoichiometry. These supercomplexes then interact with the CSM baseplate.

The above outlined hypotheses can be tested in a straightforward manner, considering that the FMO trimers are positioned atop the gRC most likely protruding from the cytoplasmic face of the cell membrane. Hence it should be possible to locate groups of such complexes using methods sensitive to surface topography, such as atomic-force microscopy or electron microscopy of negatively stained samples, in places where the CSM is detached. The latter method was recently successfully applied to the study of the native arrangement of the membrane RC-antenna complexes of *Chloroflexus (Cfx.) aurantiacus* (Bina et al. 2014).

Here, the same approach was applied to untreated fragments of cytoplasmic membrane of the GSB *Chlorobaculum tepidum*. Image data obtained from membranes were analyzed against the background of the extensive literature including electron-microscopic studies of isolated complexes and biochemical analyses. This allowed a straightforward formulation of a model of the native structure of the FMO-gRC (super)complex, distribution of the complex with respect to the chlorosome baseplate and to estimate the average RC:CSM ratio as well as the overall structure of the photosynthetic unit formed by a chlorosome and its associated ensemble of FMO-gRC complexes.

Materials and methods

C. tepidum culture

Bacteria (*C. tepidum* TLS, DSM 12025) were cultivated in 800 mL batches of modified Pfennig medium (Wahlund

et al. 1991) in 1000 mL screw-cap flasks immersed in thermostated water bath maintained at 45 °C under continuous illumination provided by 60 W incandescent light bulbs.

Isolation of membranes and purification of FMO

Cells were harvested after 3 days of cultivation by centrifugation at 6000×*g* and resuspended in 20 mM Tris–HCl, pH 8. Membranes were prepared by disruption of cells using EmulsiFlex–C5 (Avestin Inc., Canada) at 20,000 psi followed by the removal of unbroken cells by low-speed centrifugation. For the isolation of FMO, the membranes were harvested by ultracentrifugation for 2 h at 200,000×*g*, and the purification was carried out as described by Wen et al. (2009), using 0.4 M Na_2CO_3 to release FMO from the membranes. The soluble protein fraction thus obtained was dialyzed against 20 mM Tris, pH 8 for 72 h, and fractionated using gel filtration and anion exchange chromatography. The purity of the FMO preparation was judged by the OD_{271}/OD_{371} ratio, final value of which was ~0.6.

Electron microscopy

Specimens of both the purified FMO and membranes were placed on glow-discharged carbon-coated copper grids and negatively stained with 2 % uranyl acetate. Isolated proteins were visualized by JEOL JEM–2100F transmission electron microscope (JEOL Japan, using 200 kV at 20,000× magnification), and the images were recorded by a bottom-mount Gatan CCD Orius SC1000 camera. TEM of the membrane samples was performed with JEOL 1010 transmission electron microscope (JEOL, Japan) using 80 kV at 120,000× magnification. Micrographs were recorded by a CCD Sis MegaView III camera.

Projections of isolated particles were selected automatically using the EMAN 2 software (Ludtke et al. 1999), while the membrane-attached complexes were selected manually. Image analyses were carried out using RELION (Scheres 2012a) and Spider and Web (Frank et al. 1996; Shaikh et al. 2008) version 22.10. software package employing statistical approaches as described in Scheres (2012b) and van Heel and Frank (1981) and Harauz et al. (1988), respectively. While RELION provided superior resolution of the surface features in the analysis of the isolated protein sample consisting of more than 50,000 particles (Fig. 2) which were collected with higher pixel/nm ratio, in the whole membrane analysis of lower counts of less resolved particles, the reconstruction of the features of the individual particles was slightly better when using SPIDER software (Fig. 4). The grayscale-coded surface plots of the FMO trimer structures were created using a locally written MATLAB® (Mathworks Inc., USA) script.

Results and discussion

Electron microscopy of isolated FMO complex

The TEM analysis of the negatively stained purified FMO revealed a sample homogeneous with respect to the dimensions of the particles of about 8 nm, as expected for isolated FMO trimers (Fig. 1). However, the appearance of the processed particle projections was quite variable, likely due to a different tilt. This is illustrated in Fig. 2, where panels a–c show representative particle projections from a dataset out of 54,000 analyzed particles and panels d–f the approximate corresponding orientation of the X-ray structure of the FMO trimer (PDB: 3ENI, Tronrud et al. 2009). The least tilted particle, panel a, clearly showed the expected threefold symmetry, with its highly stained center corresponding to the triangular depression in the chlorosome-facing ("upper"), side of the trimer (Tsiotis et al. 1997; Wen et al. 2009), marked by the black triangle in panel d. Compared to the space-filling model, this feature appeared more pronounced than expected in the negatively stained particles. Similar unexpectedly intense staining was previously observed in the chlorosome-facing side of the RC-containing core complex of *Cfx. aurantiacus* (Bina et al. 2014). The red rings in Fig. 2d indicate the uppermost portions of the FMO trimer subunits, with the corresponding bulky features in the TEM particle indicated by arrowheads in Fig. 2a. The roughly triangular appearance with bulges in the middle of the triangle edges of the FMO trimer projection corresponded very well to the image of this complex obtained earlier using scanning transmission electron microscopy (Remigy et al. 1999).

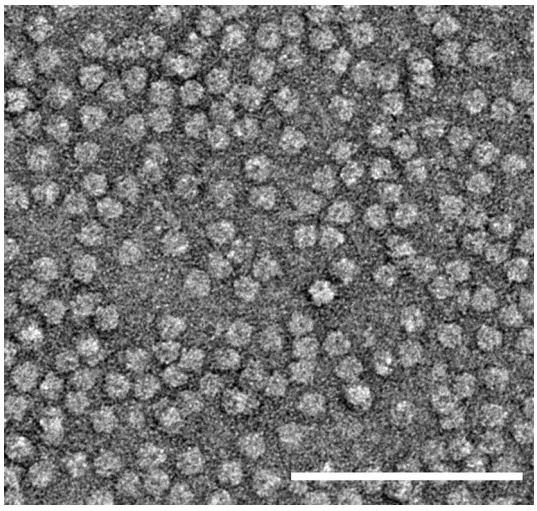

Fig. 1 Electron micrograph of a sample of purified FMO trimers stained with uranyl acetate (2 %). The scalebar corresponds to 100 nm

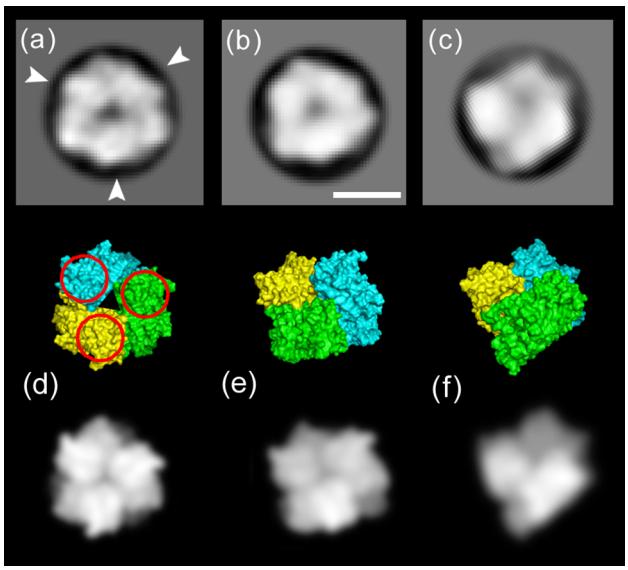

Fig. 2 Results of the single-particle analysis of isolated FMO. Panels **a–c** represent projections of differently tilted FMO trimers, with **a** being closest to the *top view*, **c** a *sideview*. The *upper*, color images in **d–f** represent the corresponding space-filling models of the structure based on the 3ENI X-ray structure, the *lower greyscale* images are the surface representations of the space-filling models. The *red rings* indicate the topmost features on the structure, likely corresponding to the features denoted by *arrows* in panel **a**. The *grey triangle* in the structure in panel **d** corresponds to the cavity formed on the interface of the subunits of the FMO trimer. *Scalebar* corresponds to 5 nm

Electron microscopy of cytoplasmic membranes

Images of the fragmented plasma membrane revealed a mixture of chlorosomes, membrane patches, and small debris as shown in Fig. 3a. As shown in the figure, certain areas of membrane were covered with particles about 20 nm in diameter with stained centers having the appearance of tetrameric assemblies of globular proteins of diameter of less than 10 nm (b–d). On rare occasions, these aggregates were even observed in connection to chlorosomes (e, f). Considering the estimated size of the subunits of the aggregates (<10 nm) and their position on the surface of the cytoplasmic membrane as well as their association to chlorosomes, we assumed that these represented supramolecular assemblies of the FMO protein. Although a water-soluble protein, FMO is rather strongly bound to the surface of the membrane, and a chemical treatment is needed to release a substantial amount of the complex into the water phase, hence it could be expected to be—at least partially—retained on the untreated membrane fragments. An unsuccessful attempt was also made to identify the FMO in the membrane samples using immunolabeling with nanogold. The primary antibody against FMO was a kind gift from Dr. Gregory Orf (Blankenship Lab, Washington University in St. Louis). However, no detailed structures could be resolved on the samples that underwent the antibody labeling procedure, and the efficiency of the FMO labeling in the membranes was low.

We thus relied on the visual identification of the FMO complex. The individual tetrameric complexes were selected manually, yielding a dataset of 1239 particles. Results of the single-particle analysis, Fig. 4a revealed clearly the four subunits of the complex. Fortunately, partial resolution of the inner structure was also possible, as shown in Fig. 4b,c, where the approximately C_3 symmetrical features in two of the tetramer subunits could be partially resolved (A and B in Fig. 4). These likely corresponded to the inner structure resolved in the isolated complex (Fig. 2a). This lent support to the hypothesis that the membrane-attached complex corresponded to a supramolecular assembly of FMO trimers. A straightforward interpretation of such structure would assume a centrally placed gRC surrounded by four FMO trimers. However, such an arrangement would likely prevent the interaction of the PscB/D subunits with the diffusible ferredoxins. Moreover, two additional protein masses positioned between pairs of FMO trimers could be tentatively located in the 4-FMO complex, as denoted by triangles in Fig. 4d. These could be interpreted as the protruding part of the gRC placed between a pair of FMO trimers, yielding a 4-FMO, 2-gRC complex in total. Then, as shown in Fig. 4d, the overall appearance of the particle would be consistent with a C_2 symmetry and it could be interpreted as a $[FMO_2\ gRC_1]_2$ supercomplex. This is shown in Fig. 4d with filled and empty symbols indicating the features corresponding to the respective $FMO_2\ gRC_1$ complexes. The proposed $[FMO_2\ gRC_1]_2$ supercomplex has two important features: (i) it leaves the iron-sulfur cluster-binding PscB/D complex exposed to the water phase, accessible to the mobile electron shuttles; (ii) it is based on the $FMO_2\ gRC_1$ structure (Remigy et al. 1999) which is arguably the best supported in the literature. The following paragraph shows such a model to be in agreement also with the recent biochemical studies.

The model of the FMO-RC complex

RC complex of GSB is formed by a homodimeric assembly of a 11-helix membrane protein (PscA) corresponding to the PsaA/B dimer of the PSI RC of oxygenic photosynthesis (Hauska et al. 2001), with which it also shares the mode of operation, both complexes performing light-driven reduction of ferredoxin via iron-sulfur clusters. Approximately in the geometrical center of the complex (when viewed perpendicular to the membrane plane), protruding into the cytoplasm in the native state, was observed a bulge (Remigy et al. 1999) formed most likely by the PscB and PscD proteins (He et al. 2014). These harbor Fe-S centers

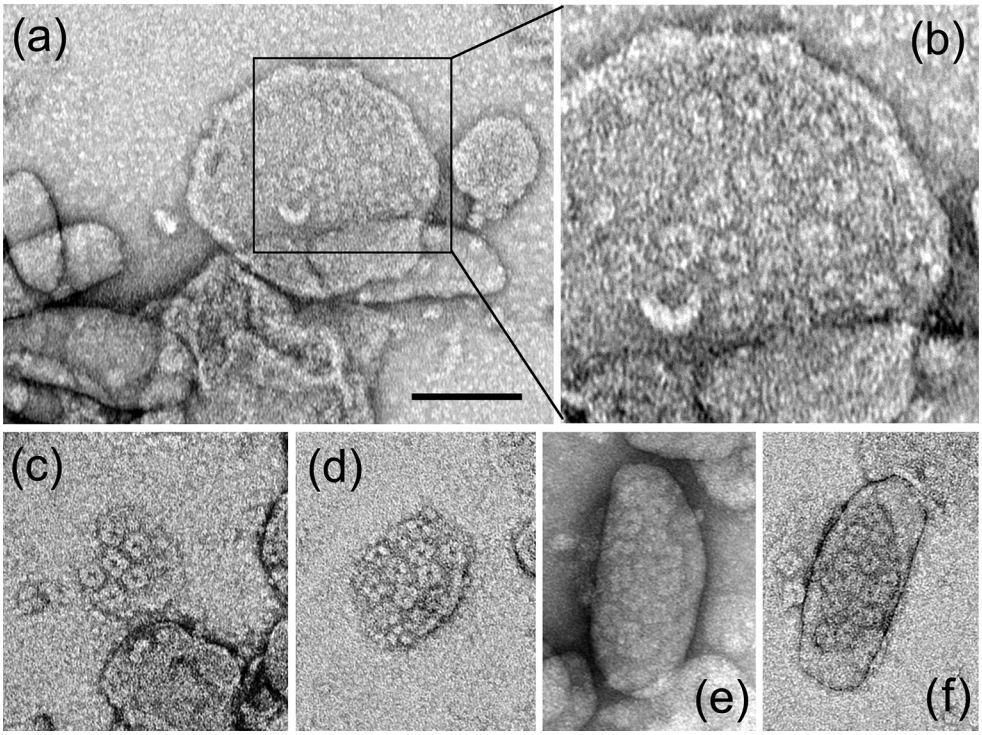

Fig. 3 Examples of the negatively stained membrane fragments isolated from the cells of the green sulfur bacterium *C. tepidum*. **a** typical appearance of the membrane sample. **b** expanded view of the region outlined in **a** containing protein aggregates. **c**, **d** further examples of membrane fragments. **e**, **f** membrane fragments with chlorosomes and protein aggregates. *Scalebar* 100 nm

and provide docking for the soluble electron transporters, respectively, in the manner of the PsaC, D and E subunits of PSI RC. Following the initial observation of the FMO trimer attached to gRC (Remigy et al. 1999), it was shown recently by means of chemical crosslinking (He et al. 2014) that both PscB and PscD are in close contact with lysines 79, 93, and 215 of the FMO. Moreover, it was shown that the lysine 79 could be positioned in the vicinity of the N-terminal end of the PscA protein. Assuming that the PscA protein of gRC adopts a tertiary structure that is similar to the PsaA/B of PSI RC, the N-terminal end of the protein is situated along the side of the complex (PDB: 1JB0, Jordan et al. 2001), approximately in position of the labeled Lys 79 residue in Fig. 5 showing the PscA vicinity. Figure 5 combines the above-described crosslinking results with the structural features observed in the particle in Fig. 4. The red rings in the structure in Fig. 5 correspond to the part of the protein responsible for the bulges labeled with arrows in Fig. 2a and red rings in Fig. 2d. The model was constructed as follows: (i) Placing the FMO trimer 'A' in the numbered position shown in Figs. 4 and 5 oriented the subunit '3' toward the center of the gRC and exposed the lysines to the PscB/D subunits. Approximating the FMO projection with a triangle (Figs. 2a, 4c), this would direct the vertices of the triangle away from the PscB/D subunits of gRC (Fig. 4), in the manner observed in the 3D reconstruction of the FMO_1 gRC_1 complex presented by Remigy et al. (1999); (ii) The FMO trimer, 'B', was placed according to the features indicated in Fig. 4. (iii) Orientations of the remaining two FMO complexes were obtained by rotating 'A' and 'B' by 180 degrees, A → D, B → C. As shown in Fig. 5, this resulted in bringing the lysine residues of these FMO trimers also into potential contact with the PscB and D. Moreover, lysine 79 now appears in the region of the putative position of the N-terminal end of the PscA protein (see above). It should be stressed that the mutual orientation of the two FMOs bound to the same gRC ('A' and 'C in Fig. 5) is not necessarily symmetrical due to the different interactions with the PscB and D subunits, which can in turn lead to different strengths of binding, consistent with the frequent loss of one FMO per gRC in isolated complexes.

The model suggested above indicates the existence of a functionally dimeric gRC complex, contrary to the established view of gRC as a monomer (Hauska et al. 2001; Remigy et al. 1999, 2002). However, as shown in Fig. 4, the separation of centers of FMOs belonging to the different gRCs is about 11 nm. The electron-microscopic structural analysis (Tsiotis et al. 1997) suggested that the dimensions of the detergent-surrounded gRC (a dimeric PscA/PscC complex) particles were less than (length × width × height) 14 × 8 × 6 nm, hence, in our

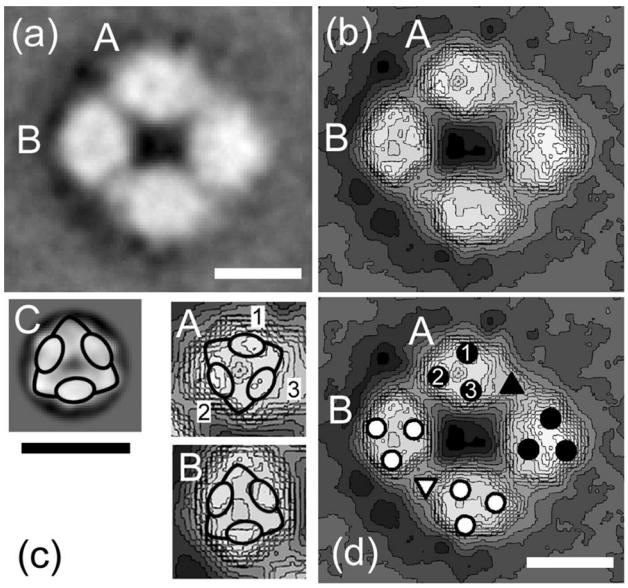

Fig. 4 Single-particle analysis of the complexes attached on the surface of the cytoplasmic membrane of *C. tepidum*. **a** representative average projection. **b** a contour plot of the same image, A and B denote subunits with resolved inner structure. These are shown enlarged in panel (**c**), along with a projection of an isolated FMO trimer, C, taken from Fig. 2a overlaid with its cartoon representation. **d** the complex with the subunits of all the four FMO trimers indicated by circles. *Triangles* correspond to the additional protein masses. *Filled* and *empty symbols* indicate the respective parts of the putative $[FMO_2gRC_1]_2$ supercomplex, each part formed by 2 FMO + 1 gRC (see text). *Scalebar* 10 nm

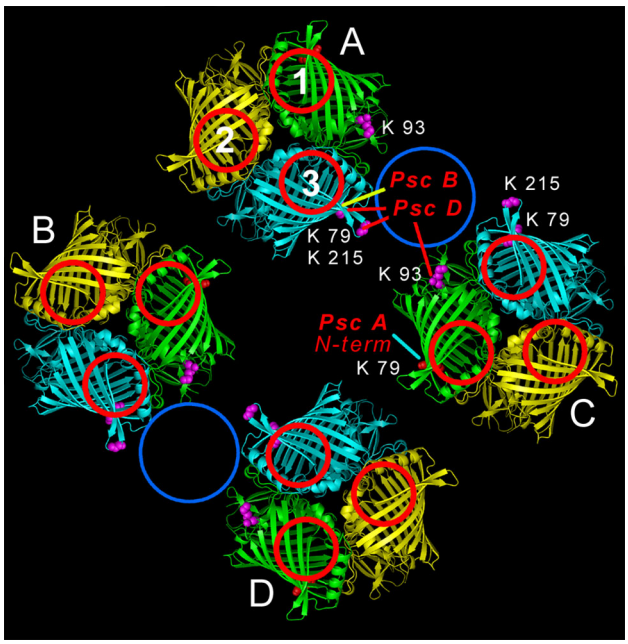

Fig. 5 A model of the 4-FMO assembly based on the particle in Fig. 4. Positions of the lysine residues (K) shown by He et al. (2014) to be in proximity to the PscA, B, and D subunits of the gRC complex are indicated as are the chemical crosslinks identified in the cited work (*straight lines*): *red*: crosslinks to PscD, *yellow*: to PscB; *cyan*: to PscA N-terminal end. The *red rings* correspond to the bulky features of the FMO trimer shown in Fig. 2. *Numbers* correspond to the labeling of the subunits in Fig. 4c and d

$[FMO_2\ gRC_1]_2$ complex, the side-to-side separation between the gRC cores is likely to exceed 3 nm, a distance much larger than, e.g., the separation of the RC complexes in the photosystem II dimer (Umena et al. 2011). This space between gRCs could be occupied by lipids, making the 2-gRC complex susceptible to detergent extraction and separation of individual gRCs. On the other hand, the question of the driving force behind the formation of the $[FMO_2\ gRC_1]_2$ complex remains as yet unresolved as is the possible role of the PscC (cytochrome) subunit in its formation.

The organization of the photosynthetic unit

In the above section, the building block of the membrane part of the photosynthetic unit was proposed in the form of a complex of C_2 symmetry comprising four FMO trimers (2 per gRC) and two gRC complexes in total ($[FMO_2\ gRC_1]_2$ supercomplex). In further step, the TEM images of negatively stained membranes were used to extract positional information to analyze the spatial distribution of supercomplexes within the cytoplasmic membrane.

The analysis of the distances to the nearest neighbor, computed from the positions of centers of 300 FMO tetramers, Fig. 6, showed a preferential distance of 24 nm between geometrical centers of $[FMO_2\ gRC_1]_2$ supercomplexes. Considering the outer dimensions of about 20 nm of the 4-FMO assembly, this leaves about 4 nm of free space between the supercomplexes, allowing for the diffusion of small mobile electron carriers, considering the outer dimension of a ferredoxin molecule of at most 3 nm (Seo et al. 2001; Dauter et al. 1997), although the diffusion of ferredoxin still likely to be hindered by the presence of protein complexes. This view implies that the ferredoxins operate in the vicinity of the membrane surface in between the membrane face and the baseplate. The height of the FMO trimers ($\sim$6 nm) appears to allow this.

The recent tomography analysis of whole-cell structure of *C. tepidum* (Kudryashev et al. 2014) reported the most common nearest neighbor distance for the gRC to be close to $\sim$10 nm, albeit with a large dispersion. This corresponded to the separation of the gRC within the $[FMO_2\text{-}gRC_1]_2$ supercomplex shown here, although in comparison to the cited work, present observations suggested a somewhat more ordered placement of gRC complexes. Considering that the determination of the center 4-FMO complex is of finite precision, the real distribution function might be even slightly narrower. The proportion of the FMO complexes retained in their native position could not

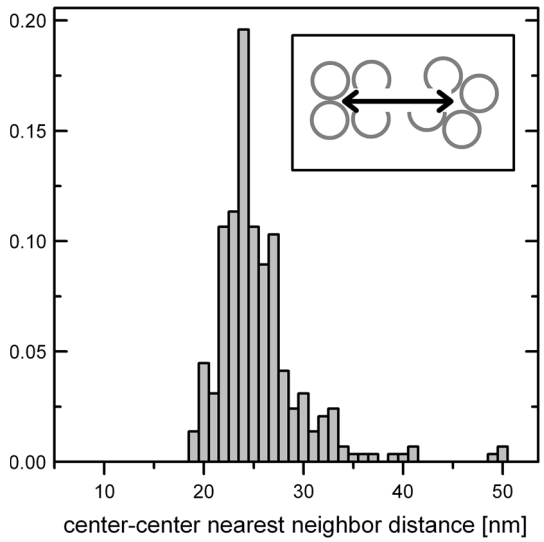

Fig. 6 The distribution of distances to the nearest neighbor for the 4-FMO complexes attached the surface of *C. tepidum* membranes ($n = 300$). The distance was measured from the center of tetramers as shown in the *inset*

be estimated as the FMO-free gRC are not likely to be identifiable on the electron micrographs, since the major part of the protein is buried in the membrane.

The typical dimensions of chlorosomes in our samples were $160 \pm 30 \times 70 \pm 12$ nm ($n = 80$). These values correspond to the baseplate area between 8800 and 10,100 nm^2, depending on whether the outline of the CSM is approximated by an ellipse (Kudryashev et al. 2014) or a rectangle capped with semicircles (Golecki and Oelze 1987; Bina et al. 2014), respectively. Using the nearest neighbor distance distribution function from Fig. 6, this yielded an estimate of the mean maximum occupancy of CSM of about 15 FMO tetramers per average baseplate, which corresponded to the total of 60 FMO trimers, about 70 % occupancy of the baseplate area by the $[FMO_2\text{-}gRC_1]_2$ complexes and as much as 30 gRCs per CSM. Thus, maintaining a conservative stoichiometry of 2 FMO per gRC, these values compare very well with the earlier CSM:gRC estimates of 25-40 (Frigaard et al. 2003; Frigaard and Bryant 2006; Hauska et al. 2001), but the number of FMOs per CSM is much smaller compared to 150–200 suggested by Frigaard et al. (2003). However, these numbers were based on estimates of partitioning of BChl *a* between the CSM and FMO, thus strongly dependent on correct estimation of BChl *a* content of the CSM baseplate (see Bina et al. 2014; Wittmershaus et al. 1988). It must be kept in mind that the stoichiometries derived in the present work are based on the particle spacing and do not take into account the possibility of the presence of any free, unbound FMO, which is a soluble protein, or possible chlorosome-free but FMO-containing areas of membrane that may precede the formation of the complete photosynthetic unit (Pedersen et al. 2010) and thus may differ from the bulk estimates of FMO and CSM concentrations. On the other hand, for the FMO trimer of ~8 nm in diameter, i.e., having an area of 50 nm^2, the absolute upper limit of FMO:CSM ratio is 200, not allowing for any free space left between FMO complexes nor the observed tetrameric assembly; thus, it is not in agreement with the present observations.

Moreover, based on the present results, the earlier views presented, e.g., by Frigaard et al. (2003), that the gRC complexes are placed around the edge of the chlorosome, can be abandoned (Fig. 3). Instead, the apparent problem of accessibility of the gRC to the mobile electron carriers is solved by spacing of the $[FMO_2\ gRC_1]_2$ complexes (Fig. 6), although the question of what determines the spacing during the development of the supramolecular structure remains to be addressed. Finally, it hereby appears that the supramolecular organization of FMO stems primarily from its association with gRC rather than from the highly ordered structure of the baseplate.

Comparison to chlorosome-containing Chloroflexi

At present, there are three known phyla comprising phototrophic bacteria employing chlorosomes: *Chlorobi*, *Chloracidobacteria,* and *Chloroflexi*.

The photosynthetic apparatus of *Chloracidobacteria* is similar to GSB, including the type I RC and FMO (Bryant et al. 2007; Tsukatani et al. 2010), leaving *Chloroflexi* as the only fundamentally different example of CSM use, i.e., a system coupling CSM to the type II, quinone-reducing, RC of the purple-bacterial type. This system operates without any connecting element corresponding to FMO, since it does not require the cytoplasmic side of the RC to be accessible from the water phase (Blankenship 2014; also see Dostal et al. 2014), relying instead on the intramembrane electron transport by quinones. It should be noted that the *Cfx. aurantiacus* RC also lacks the H-subunit (Blankenship et al. 1983) protruding above the membrane plane (Fotiadis et al. 2004), which is found in typical RCs of purple bacteria.

The in vivo structure of the *Chloroflexus aurantiacus* photosynthetic unit was analyzed recently (Bina et al. 2014) allowing for a comparison of the two structures, shown in cartoon in Fig. 7; a corresponds to the photosynthetic unit of *C. tepidum* based on the present results; b shows the CSM-RC-B808–866 assembly of *Cfx. aurantiacus* based on the paper of Bina et al. (2014). The typical number of RC-antenna complexes per CSM in *Cfx. aurantiacus* was found to be about 11, compared to the ~30 gRC complexes in *C. tepidum*. However, the dimensions of CSM of *Cfx. aurantiacus* were found to be smaller than in the case of *C. tepidum*, the average length and width of

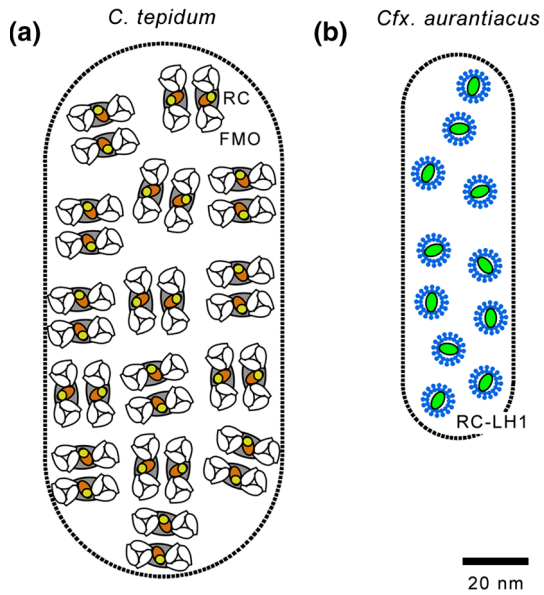

Fig. 7 A cartoon comparing the structure of an average photosynthetic unit (CSM-inner antenna-RC) of the two types of CSM-containing bacteria, derived from electron-microscopic analysis of negatively stained membranes. **a** green sulfur bacterium *C. tepidum* (this work). **b** filamentous anoxygenic phototroph *Cfx. aurantiacus* (Bina et al. 2014). LH1 denotes the B808–B866 complex, core antenna of *Chloroflexus*

negatively stained chlorosomes were about 118 × 34 nm (Bina et al. 2014; Golecki and Oelze 1987). Comparing the areas of chlorosomes, ~9000 and 3200 nm^2 for *C. tepidum* and *Cfx. aurantiacus*, respectively, one sees that for about 2.5–3-fold larger baseplate area, there is a proportional increase of total number of RC complexes per CSM, maintaining approximately the same CSM area per RC ratio in both systems. However, it is possible that the RC:CSM ratio is variable in response to changing environmental conditions such as irradiance. We consider the extent of such plasticity to be a matter of further research.

Conclusions

This is to our knowledge the first study dealing directly with the native organization of the photosynthetic membrane of GSB on the intermediate scale. Making use of the wealth of the already available biochemical, structural, and biophysical data, the focus of the present work was placed on image analysis. Positions of FMO trimers on the surface of the membrane were identified allowing for the analysis of not only the structure but also spatial distribution of the native assemblies of FMO proteins and their association with the gRC. A model of the native complex was proposed consisting of a total of four FMO trimers and two gRC. Analysis of distribution of the supercomplexes in the membrane led to the mean estimate of about 30 gRC and 60 FMO complexes per average chlorosome.

Acknowledgments We are indebted to Dr. Jakub Pšenčík (Charles University in Prague) for fruitful discussions and to Dr. Gregory Orf and Dr. Robert Blankenship (Washington University in St. Louis) for critical reading of the manuscript. The research was supported by Czech Science Foundation project P501/12/G055 and institutional support RVO:60077344. Skilled technical assistance of František Matoušek is also gratefully acknowledged.

Compliance with ethical standards

Conflict of Interest The authors declare that they have no conflict of interest.

References

Bina D, Blankenship RE (2013) Chemical oxidation of the FMO antenna protein from *Chlorobaculum tepidum*. Photosynth Res 116:11–19

Bina D, Gardian Z, Litvin R, Vacha F (2014) Supramolecular organization of photosynthetic membrane proteins in the chlorosome-containing bacterium *Chloroflexus aurantiacus*. Photosynth Res 122:13–21

Blankenship RE (2014) Molecular mechanisms of photosynthesis, 2nd edn. Wiley-Blackwell, Oxford, pp 79–82

Blankenship RE, Feick R, Bruce BD, Kirmaier C, Holten D, Fuller RC (1983) Primary photochemistry in the facultative green photosynthetic bacterium *Chloroflexus aurantiacus*. J Cell Biochem 22:1097–4644

Bryant DA, Costas AMG, Maresca JA, Chew AGM, Klatt CG, Bateson MM, Tallon LJ, Hostetler J, Nelson WC, Heidelberg JF, Ward DM (2007) *Candidatus* Chloracidobacterium thermophilum: an aerobic phototrophic acidobacterium. Science 317:523–526

Cartron ML, Olsen JD, Sener M, Jackson PJ, Brindley AA, Qian P, Dickman MJ, Leggett GJ, Schulten K, Hunter CN (2014) Integration of energy and electron transfer processes in the photosynthetic membrane of *Rhodobacter sphaeroides*. Biochim Biophys Acta 1837:1769–1780

Dauter Z, Wilson KS, Sieker LC, Meyer J, Moulis JM (1997) Atomic resolution (0.94 Å) structure of *Clostridium acidurici* ferredoxin. Detailed geometry of [4fe-4 s] clusters in a protein. Biochemistry 36:16065–16073

Dostal J, Vacha F, Psencik J, Zigmantas D (2014) 2D electronic spectroscopy reveals excitonic structure in the baseplate of a chlorosome. J Phys Chem Lett 5:1743–1747

Fenna RE, Matthews BW (1975) Chlorophyll arrangement in a bacteriochlorophyll protein from *Chlorobium limicola*. Nature 258:573–577

Fotiadis D, Qian P, Philippsen A, Bullough PA, Engel A, Hunter CN (2004) Structural analysis of the reaction center light-harvesting complex I photosynthetic core complex of *Rhodospirillum rubrum* using atomic force microscopy. J Biol Chem 279:2063–2068

Frank J, Radermacher M, Penczek P, Zhu J, Li YH, Ladjadj M, Leith A (1996) SPIDER and WEB: processing and visualization of images in 3D electron microscopy and related fields. J Struct Biol 116:190–199

Frigaard N-U, Bryant DA (2006) Chlorosomes: antenna organelles in green photosynthetic bacteria. In: Shively JM (ed) Microbiology monographs, vol 2., Complex intracellular structures in prokaryotes. Springer, Berlin, pp 79–114

Frigaard N-U, Chew AGM, Li H, Maresca JA, Bryant DA (2003) *Chlorobium tepidum*: insights into the structure, physiology, and metabolism of a green sulfur bacterium derived from the complete genome sequence. Photosynth Res 78:93–117

Golecki JR, Oelze J (1987) Quantitative relationship between bacteriochlorophyll content, cytoplasmic membrane structure and chlorosome size in *Chloroflexus aurantiacus*. Arch Microbiol 148:236–241

Griesbeck C, Hager-Braun C, Rogl H, Hauska G (1998) Quantitation of P840 reaction center preparations from *Chlorobium tepidum*: chlorophylls and FMO-protein. Biochim Biophys Acta 1365:285–293

Harauz G, Boekema EJ, van Heel M (1988) Statistical image analysis of electron micrographs of ribosomal subunits. Methods Enzymol 164:35–49

Hauska G, Schoedl T, Remigy H, Tsiotis G (2001) The reaction center of green sulfur bacteria. Biochim Biophys Acta 1507:260–277

He G, Zhang H, King JD, Blankenship RE (2014) Structural analysis of the homodimeric reaction center complex from the photosynthetic green sulfur bacterium *Chlorobaculum tepidum*. Biochemistry 53:4924–4930

Hohmann-Marriott MF, Blankenship RE (2007a) Variable fluorescence in green sulfur bacteria. Biochim Biophys Acta 1767:106–113

Hohmann-Marriott MF, Blankenship RE (2007b) Hypothesis on chlorosome biogenesis in green photosynthetic bacteria. FEBS Lett 581:800–803

Hohmann-Marriott MF, Blankenship RE, Roberson RW (2005) The ultrastructure of *Chlorobium tepidum* chlorosomes revealed by electron microscopy. Photosynth Res 86:145–154

Jordan P, Fromme P, Witt HT, Klukas O, Saenger W, Krauss N (2001) Three-dimensional structure of cyanobacterial photosystem I at 2.5 Å resolution. Nature 411:909–917

Kudryashev M, Aktoudianaki A, Dedoglou D, Stahlberg H, Tsiotis G (2014) The ultrastructure of *Chlorobaculum tepidum* revealed by cryo-electron tomography. Biochim Biophys Acta 1837:1635–1642

Ludtke SJ, Baldwin PR, Chiu W (1999) EMAN: semiautomated software for high-resolution single-particle reconstructions. J Struct Biol 128:82–97

Majumder ELW, Olsen JD, Qian P, Collins AM, Hunter CN, Blankenship RE (2015) Supramolecular organization of photosynthetic complexes in membranes of *Roseiflexus castenholzii*. Photosynth Res. doi:10.1007/s11120-015-0179-9

Oelze J, Golecki JR (1995) Membrane and chlorosomes of green bacteria: structure, composition and development. In: Blankenship RE, Madigan MT, Bauer CE (eds) Anoxygenic photosynthetic bacteria, vol 2. Kluwer Academic Publishers, Dordrecht/Boston/London, pp 259–272

Olbrich C, Jansen TLC, Liebers J, Aghtar M, Strumpfer J, Schulten K, Knoester J, Kleinekathofer U (2011) From atomistic modeling to excitation transfer and two-dimensional spectra of the FMO light-harvesting complex. J Phys Chem B 115:8609–8621

Orf GS, Blankenship RE (2013) Chlorosome antenna complexes from green photosynthetic bacteria. Photosynth Res 116:315–331

Pedersen MO, Linnanto J, Frigaard NU, Nielsen NC, Miller M (2010) A model of the protein pigment baseplate complex in chlorosomes of photosynthetic green bacteria. Photosynth Res 104:233–243

Psencik J, Butcher SJ, Tuma R (2014) Chlorosomes: structure, function and assembly. In: Hohmann-Marriott MF (ed) The structural basis of biological energy generation. Advances in photosynthesis and respiration, vol 39. Springer, New York, pp 77–109

Remigy H, Fotiadis D, Hauska G, Wolpensinger B, Muller SA, Engel A, Tsiotis G (1998) Evidence for the association of three FMO subunits per reaction center of *Chlorobium tepidum* by scanning transmission electron microscopy. In: Garab G (ed) Photosynthesis: mechanisms and effects, vol 1. Kluwer Academic Publishers, Dordrecht, pp 125–128

Remigy HW, Stahlberg H, Fotiadis D, Müller SA, Wolpensinger B, Engel A, Hauska G, Tsiotis G (1999) The reaction center complex from the green sulfur bacterium *Chlorobium tepidum*: a structural analysis by scanning transmission electron microscopy. J Mol Biol 290:851–858

Remigy HW, Hauska G, Muller SA, Tsiotis G (2002) The reaction centre from green sulfur bacteria: progress towards structural elucidation. Photosynth Res 71:91–98

Scheres SHW (2012a) RELION: implementation of a Bayesian approach to cryo-EM structure determination. J Struct Biol 180:519–530

Scheres SHW (2012b) A Bayesian view on Cryo-EM structure determination. J Mol Biol 415:406–418

Scheuring S, Levy D, Rigaud J-L (2005) Watching the components of photosynthetic bacterial membranes and their in situ organisation by atomic force microscopy. Biochim Biophys Acta 1712:109–127

Schmidt am Busch M, Muh F, Madjet ME, Renger T (2011) The eighth bacteriochlorophyll completes the excitation energy funnel in the FMO protein. J Phys Chem Lett 2:93–98

Seo D, Tomioka A, Kusumoto N, Kamo M, Enami I, Sakurai H (2001) Purification of ferredoxins and their reaction with purifed reaction center complex from the green sulfur bacterium *Chlorobium tepidum*. Biochim Biophys Acta 1503:377–384

Shaikh TR, Gao H, Baxter WT, Asturias FJ, Boisset N, Leith A, Frank J (2008) SPIDER image processing for single-particle reconstruction of biological macromolecules from electron micrographs. Nat Protoc 3:1941–1974

Sprague SG, Staehelin LA, Dibartolomeis MJ, Fuller RC (1981) Isolation and development of chlorosomes in the green bacterium *Chloroflexus aurantiacus*. J Bacteriol 147:1021–1031

Swarthoff T, Amesz J (1979) Photochemically active pigment-protein complexes from the green photosynthetic bacterium *Prosthecochloris aestuarii*. Biochim Biophys Acta 548:427–432

Tronrud DE, Schmid MF, Matthews BW (1986) Structure and X-ray amino acid sequence of a bacteriochlorophyll a protein from *Prosthecochloris aestuarii* refined at 1.9 Å resolution. J Mol Biol 188:443–454

Tronrud DE, Wen J, Gay L, Blankenship RE (2009) The structural basis for the difference in absorbance spectra for the FMO antenna protein from various green sulfur bacteria. Photosynth Res 100:79–87

Tsiotis G, Hager-Braun C, Wolpensinger B, Engel A, Hauska G (1997) Structural analysis of the reaction center from green sulfur bacterium *Chlorobium tepidum*. Biochim Biophys Acta 1322:163–172

Tsukatani Y, Miyamoto R, Itoh S, Oh-oka H (2004) Function of a PscD subunit in a homodimeric reaction center complex of the photosynthetic green sulfur bacterium *Chlorobium tepidum* studied by insertional gene inactivation - Regulation of energy transfer and ferredoxin-mediated NADP(+) reduction on the cytoplasmic side. J Biol Chem 279:51122–51130

Tsukatani Y, Wen JZ, Blankenship RE, Bryant DA (2010) Characterization of the FMO protein from the aerobic chlorophototroph, *Candidatus* Chloracidobacterium thermophilum. Photosynth Res 104:201–209

Umena Y, Kawakami K, Shen JR, Kamiya N (2011) Crystal structure of oxygen-evolving photosystem II at a resolution of 1.9 Å. Nature 473:55–60

van Gemerden H, Mas J (1995) Ecology of phototrophic sulfur bacteria. In: Blankenship RE, Madigan MT, Bauer CE (eds)

Anoxygenic photosynthetic bacteria. Kluwer Academic Publishers, Dordrecht/Boston/London, pp 259–272

van Heel M, Frank J (1981) Use of multivariate statistics in analyzing the images of biological macromolecules. Ultramicroscopy 6:187–194

Wahlund TM, Woese CR, Castenholz RW, Madigan MT (1991) A thermophilic green sulfur bacterium from New Zealand hot-springs, *Chlorobium tepidum* sp. nov. Arch Microbiol 156:81–90

Wen J, Zhang H, Gross ML, Bankenship RE (2009) Membrane orientation of the FMO antenna protein from *Chlorobaculum tepidum* as determined by mass spectrometry-based footprinting. Proc Natl Acad Sci USA 106:16134–16139

Wen J, Zhang H, Gross ML, Blankenship RE (2011) Native electrospray mass spectrometry reveals the nature and stoichiometry of pigments in the FMO antenna protein. Biochemistry 50:3502–3511

Wittmershaus BP, Brune DC, Blankenship RE (1988) Energy transfer in *Chloroflexus aurantiacus*: effects of temperature and anaerobic conditions. In: Scheer H, Schneider S (eds) Photosynthetic light-harvesting systems. Walter de Gruyter, Berlin, pp 543–554

Zhou W, LoBrutto R, Lin S, Blankenship RE (1994) Redox effects on the bacteriochlorophyll a-containing Fenna–Matthews–Olson protein from *Chlorobium tepidum*. Photosynth Res 41:89–96